Binding in Thiophene and Benzothiophene Dimers Investigated By Density Functional Theory with Dispersion-Correcting Potentials

Iain D. Mackie,[†] Sean A. McClure,[‡] and Gino A. DiLabio[†,*]

National Institute for Nanotechnology, National Research Council of Canada, 11421 Saskatchewan Drive, Edmonton, Alberta, Canada T6G 2M9 and; Department of Chemistry, University of Alberta, 11227 Saskatchewan Drive, Edmonton, Alberta, Canada T6G 2G2

Received: February 3, 2009; Revised Manuscript Received: March 5, 2009

We report the use of a newly developed dispersion-corrected density functional approach to study noncovalent binding in a series of thiophene and benzothiophene dimers. These are of interest in both petrochemistry and molecular electronics. We find increasing influence of dispersion forces over dipole interactions as the number of benzene moieties increases from 0 (thiophene) to 3 (tribenzothiophene). Binding in dimers of thiophene was benchmarked vs previously published CCSD(T) data (*J. Am. Chem. Soc.* **2002**, *124*, 12200). We have determined the fully optimized geometries and energies of 15 dimers of thiophene, 26 dimers of benzothiophene, 10 of dibenzothiophene, and 11 of tribenzothiophene using B971/6-31+G(d,p) with dispersion-correcting potentials (DCPs). These represent a mixture of T-shaped, tilted-T-shaped, π-stacked, and coplanar structures. For thiophene we find the lowest energy T-shaped and π-stacked dimers to bind by 3.0 and 2.5 kcal/mol, respectively. However, for benzothiophene the lowest energy structure is π-stacked with binding energy, BE = 5.8 kcal/mol, which compares to the most bound T-shaped dimer, BE = 4.1 kcal/mol. This difference between π-stacked and T-shaped dimer binding increases further going to dibenzothiophene and tribenzothiophene (difference = ca. 6.0 and 6.7 kcal/mol, respectively). When calculations without dispersion corrections are performed on the dimer structures, many display significant changes in structural motif and reductions in binding energies of up to 80%. Therefore, the inclusion of dispersion corrections, for example, through the use of DCPs, is essential in describing the potential energy landscape of these complexes.

1. Introduction

Thiophenes are an interesting class of molecules in that they play important roles in such diverse areas as petrochemistry and in molecular electronics. The significance of thiophenes in oil upgrading arises from their role as constituents of asphaltenes and from their use as models for asphaltene resins. These resins are intermediate fractions of crude that bind to the asphaltene component.[1] From the oil-upgrading standpoint, asphaltene aggregation, which is driven primarily by noncovalent interactions, is extremely problematic.

While noncovalent interactions are deleterious in oil sands processing, these same forces are critical to the favorable self-association in molecular electronics systems, such as conjugated polythiophenes[2] (other examples include graphene layers[3] or pentacene[4]), which result in their interesting properties.

The structural aspects of thiophene aggregation are of interest to us because understanding how these molecules bind noncovalently can provide an understanding of how disaggregation of more complex asphaltene molecules might be achieved. They can also provide insight into the factors that affect electronic overlap that is critical to the functionality of electronic materials.

In the present work, we discuss the binding that occurs between four thiophene monomers, shown in Scheme 1. The monomers include simple thiophene and mono-, di-, and tribenzothiophenes. We expect that the dimerization of these thiophenes will be driven by dipole forces and by dispersion interactions.[5] The relative strengths of these forces will ultimately determine the most stable dimer structures and the general features of the potential energy surfaces associated with dimerization. The structures and binding energies of the dimers are calculated using a recently developed dispersion-corrected density functional theory approach,[6] which was benchmarked against previously reported high-level data for the thiophene dimer.[7] Our past efforts[6,8,9] have shown that dispersion interactions can be computed accurately by introducing atom-centered, dispersion-correcting potentials. With this approach we are able to utilize relatively small basis sets, without faltering on the accurate determination of molecular binding energies or structure.

SCHEME 1: Dimerization of Thiophenes Studied in the Present Work

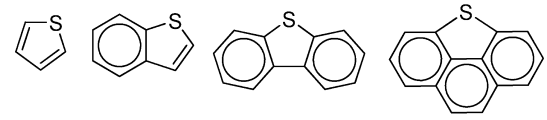

1 **2** **3** **4**

2. Methodology

Quantum mechanics can provide invaluable insight into chemical properties of molecular systems; however, it is not without its challenges. For the study of aggregation of **1**−**4** into dimers (dimers are henceforth referred to as $\mathbf{1_2}$−$\mathbf{4_2}$), dispersion will play an important role. These interactions are notoriously difficult to model. For example, the MP2 method (the least computationally intensive and most commonly applied wave

* To whom correspondence should be addressed. Fax: +1 780 641-1601. E-mail: gino.dilabio@nrc.ca.
† National Research Council of Canada.
‡ University of Alberta.

10.1021/jp901001w CCC: $40.75 © 2009 American Chemical Society
Published on Web 04/09/2009

function technique) tends to overestimate dispersion interaction, even with the use of large basis sets.[10] In any case, the large size of the dimers under study in the present work (especially $\mathbf{4_2}$) precludes the use of methods such as MP2. More accurate methods, such as coupled-cluster techniques, are even more computationally intensive and can only be applied to very small systems. This leaves density functional theory (DFT) as the only practical alternative. However, DFT is notoriously poor at describing dispersion interactions because most DFTs do not contain the correct dispersion physics. In many cases, DFTs predict overly repulsive, long-range behavior. Some headway has been made in correcting this shortcoming of DFT either through the formulation of new functionals,[11−14] by introducing empirical[15,16] or ab initio[17] long-range potential corrections, or through the use of planewave, nonlocal pseudopotentials[18] (e.g., based upon Goedecker-type[19] potentials).

Our own approach to the dispersion problem in DFT involves the use of Gaussian functions. These dispersion-correcting potentials (DCPs), which are effective-core type local potentials, correct the erroneous long-range behavior of DFTs. This method was based on one developed to produce atom-centered quantum capping potentials,[20] which are a convenient way to circumvent problems associated with link atoms in quantum mechanical/molecular mechanics modeling[21] and for calculating vibrations in truncated systems.[22] It is important to note that DCPs do not introduce the "correct physics" for dispersion binding into the DFTs to which they are applied. Rather, DCPs change the potentials in which the electrons move such that the correct dispersion binding behavior is approximated.

The DCP approach can be employed in conjunction with standard computational programs and utilize all of the features of these packages, e.g., implicit solvation models, frequency calculations, etc., as implemented in ab initio codes such as GAUSSIAN 03.[23] Note that DCPs were developed such that errors due to basis set incompleteness need not be calculated.[24] The DCPs used in this work were designed for carbon atoms, though they can also be developed for other atoms. Our results will nevertheless show that we do not require DCPs for H or S atoms to provide a good treatment of dispersion binding in thiophene dimers.

Reference 8 describes the design of DCPs for several density functionals, including the popular B3[24]LYP.[25] We found that B86-based functionals with DCPs predict the properties of dispersion-bound systems with greater accuracy than B88-based functionals such as B3LYP.[6,8] For example, percent absolute deviations of 13.8 and 23.3 are found for a series of hydrocarbon dimers using B971 and B3LYP, respectively, with 6-31+G(d,p) basis sets and optimized DCPs.[8] In the present work, DCPs have been employed in conjunction with B971[26] and PBE[27] density functionals and 6-31+G(d,p) basis sets. Optimized coefficients for the DCPs for both density functionals were taken from ref 8 and used as is. The DCPs have been applied to all of the carbon atoms in the systems studied. We describe these dispersion-correcting DFT methods as B971/6-31+G(d,p)-DCP and PBE/6-31+G(d,p)-DCP. These combinations of methods, basis sets and DCPs have been shown to provide accurate molecular geometries and complex binding energies with minimal computational effort.[6,8] As an illustration of how DCPs correct the erroneous dispersion binding predicted by the B971 functional, Figure 1 shows the potential energy surface (PES) for a thiophene dimer constrained to C_{2v} symmetry. Note that the DCPs do not completely correct the long-range repulsion predicted by B971, c.f., points on the PES near 7.4 Å, which are ca. 0.04 kcal/mol above the dissociation limit. However, a substantial improvement in the dispersion binding and intermonomer separation are obtained.

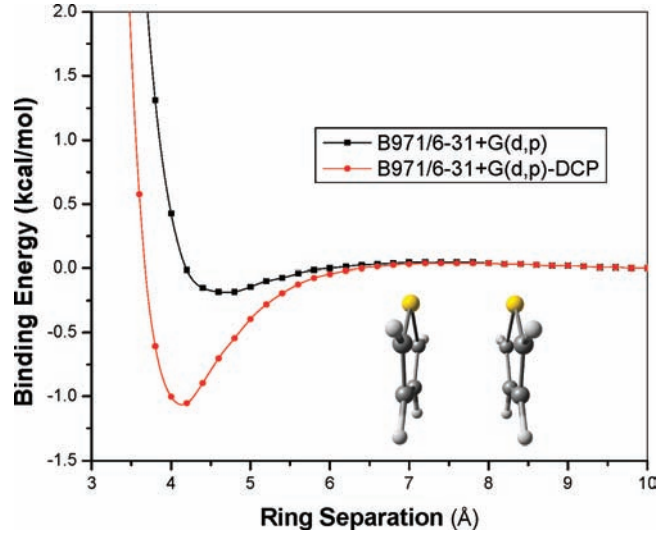

Figure 1. B971/6-31+G(d,p) potential energy surface for dimer $\mathbf{1_2a'}$ computed with and without carbon DCPs. The high-level results of ref 7 gives a binding energy of 1.32 kcal/mol and the intermonomer distance as ca. 4.0 Å.

Unless otherwise noted, all calculations were performed with the GAUSSIAN-03 suite of programs. Optimized Cartesian coordinates can be found in the Supporting Information. A sample input file illustrating the use of DCPs is also given in the SI. The binding energies reported do not include corrections for zero-point energy.

2.1. Comparison of DCP to Published High-Level Wave Function Results. Tsuzuki and co-workers reported the structures and energies of 17 different thiophene dimers, labeled $\mathbf{1_2a'}-\mathbf{1_2q'}$.[7] The prime symbol denotes that the dimers are optimized under some symmetry constraint. In their study, Tsuzuki et al. used the optimized geometries of the monomer to perform a series of single-point calculations for each dimer until a minimum energy structure was obtained. Energy calculations were performed using a composite wave function scheme utilizing a combination of MP2 and CCSD(T) to estimate the CCSD(T) limit energies. This scheme is purported to reproduce high-level, wave function results.[7] The structures reported in ref 7 provide good starting points for the present study and allow us to assess the ability of our DCP approach to predict dispersion binding for thiophenes. We optimized each dimer structure using the symmetry constraints imposed in the work by Tsuzuki et al.[7] and performed frequency calculations to determine whether they are an energy minimum, transition state or higher order saddle point. In Table 1, we compare the binding energies we calculate to those reported in ref 7. These partially optimized structures are shown in Figure 2.

Dimers $\mathbf{1_2a'}-\mathbf{1_2c'}$ correspond to π-stacked (sandwich) structures, while $\mathbf{1_2d'}-\mathbf{1_2j'}$ can be described as T-shaped, and $\mathbf{1_2k'}-\mathbf{1_2q'}$ are coplanar. Table 1 compares the binding energies of $\mathbf{1_2a'}-\mathbf{1_2q'}$, determined using B971 and PBE to the estimated CCSD(T)-level data of ref 7. We find there to be excellent agreement between these methods. B971 and PBE with DCPs give essentially the same results, with total mean absolute deviations (MAD) of 0.16 and 0.17 kcal/mol, respectively. These represent mean percent absolute deviations of 18.2 and 31.2%, with much of the error arising from coplanar dimers.

The BEs for the π-stacked dimers $\mathbf{1_2a'}-\mathbf{1_2c'}$ calculated by B971/6-31+G(d,p)-DCP underestimate those determined by

TABLE 1: Signed Deviations (SD, kcal/mol) and Percent Absolute Deviations (%AD) of Binding Energies Compared to High-Level Data for a Series of 17 Symmetry-Constrained Thiophene Dimers Using Method/6-31+G(d,p) with Carbon DCPs[a]

	B971		PBE		High-level[b]
dimer $\mathbf{1}_2$	SD	%AD	SD	%AD	BE
		π-stacked			
a′	−0.22	16.7	−0.29	22.0	1.32
b′	−0.26	16.4	−0.34	21.4	1.59
c′	0.11	7.1	0.13	8.3	1.56
		T-Shaped			
d′	−0.26	13.9	−0.19	10.2	1.87
e′	0.43	20.9	0.26	12.6	2.06
f′	−0.27	16.2	−0.27	16.2	1.67
g′	0.29	14.1	0.23	11.2	2.05
h′	0.15	6.6	0.09	3.9	2.28
i′	0.05	1.9	−0.01	0.4	2.60
j′	0.18	7.8	0.23	10.0	2.31
Coplanar					
k′	−0.06	8.2	−0.14	19.2	0.73
l′	−0.07	18.9	−0.06	16.2	0.37
m′	−0.14	34.1	−0.13	31.7	0.41
n′	0.05	7.8	0.03	4.7	0.64
o′	−0.07	16.7	0.06	14.3	0.42
p′	−0.12	85.7	0.32	228.6	0.14
q′	−0.01	16.7	−0.06	100.0	0.06
M(%)AD (**a′**−**c′**)	0.20	13.4	0.25	17.2	
M(%)AD (**d′**−**j′**)	0.23	11.6	0.18	9.2	
M(%)AD (**k′**−**q′**)	0.07	26.9	0.11	59.2	
M(%)AD (total)	0.16	18.2	0.17	31.2	

[a] Carbon DCP exponents (ref 8) are $\xi_1 = 0.08$ and $\xi_2 = 0.12$. Optimized carbon DCP coefficients as given in Table 1 of ref 8. B971: $c_1 = -0.001438$, $c_2 = 0.003475$; PBE: $c_1 = -0.001550$, $c_2 = 0.003300$. Mean (percent) absolute deviations (MAD, kcal/mol and M%AD in %) from the high-level data are given at the bottom of the table. [b] High-level data from ref 7 with pictorial representations of dimers $\mathbf{1_2a'}-\mathbf{1_2q'}$ therein. Figure 2 shows the structures we obtain following symmetry-constrained geometry optimizations.

TABLE 2: B971/6-31+G(d,p)-DCP Calculated Binding Energies (BE, kcal/mol) and Some Structural Data for Fully Optimized Thiophene Dimers

dimer $\mathbf{1}_2$	BE	angle(deg)[b]	r (Å)[c]
	π-stacked		
a	2.5	0.4	3.92
l[a]	2.5	0.8	3.91
c[a]	2.2	9.1	4.05
b[a]	1.8	3.8	4.19
	T-Shaped		
p	3.0	88.2	4.79
d	3.0	85.6	4.78
i[d]	2.7	90.0	4.92
j	2.6	84.3	4.85
e[d]	2.5	90.0	4.90
o	2.5	87.2	4.88
h[d]	2.4	90.0	4.92
g	2.4	88.5	4.83
f	1.9	76.0	4.89
q	1.8	87.8	5.75
	Coplanar		
n	0.7	0.0	6.89

[a] DCPs required to find this minimum.[28] [b] Angle between ring planes. [c] Distance between geometric ring centers. [d] Minima correspond to structures described in Table 1 and Figure 2.

Tsuzuki et al.[7] by an average signed deviation (SD) of 0.12 kcal/mol. The most strongly bound of the π-stacked structures, $\mathbf{1_2c'}$, has a calculated BE = 1.67 kcal/mol, a value that is higher than the ab initio value by 0.11 kcal/mol (ca. 7%). Errors associated with BEs calculated using PBE/6-31+G(d,p)-DCP are slightly larger than the analogous B971 BEs.

The B971/6-31+G(d,p)-DCP BEs for the T-shaped dimers $\mathbf{1_2d'}-\mathbf{1_2j'}$ are, on average, slightly overestimated (average SD 0.08 kcal/mol) compared to the values reported in ref 7. The largest error in BE for a T-shaped structure is found for $\mathbf{1_2e'}$, which is predicted to be 0.43 kcal/mol (ca. 21%) too high. Errors in PBE/6-31+G(d,p)-DCP predicted BEs for the T-shaped dimers are slightly lower than those obtained with B971/6-31+G(d,p)-DCP.

The binding calculated for the coplanar thiophene dimers, $\mathbf{1_2k'}-\mathbf{1_2q'}$, is consistently less than 1 kcal/mol, as reported by Tsuzuki et al.[7] Our results indicate the maximum binding in such systems to equal 0.69 kcal/mol with B971/6-31+G(d,p)-DCP (for structure $\mathbf{1_2n'}$) which is in excellent agreement with the value of 0.64 kcal/mol from ref 7. In general, the absolute errors in the B971/6-31+G(d,p)-DCP and PBE/6-31+G(d,p)-DCP predicted binding energies for the coplanar structures are lower than those found for the π-stacked and T-shaped dimers. However, percent errors in BE are fairly large, primarily because the BEs for the coplanar structures tend to be very low. MAD/%ADs for these coplanar species are 0.07/26.9 and 0.11/59.2, respectively.

The data presented in Table 1 justifies the use of B971/6-31+G(d,p)-DCP for the remainder of this study. The overall average signed deviation in the B971/6-31+G(d,p)-DCP predicted BEs from those reported in ref 7 is only −0.01 kcal/mol, indicating that our calculated data bracket the high-level results. This shows that π-stacked and T-shaped dimers are treated in a reasonably consistent fashion. It is worthwhile pointing out that we do not require DCPs for the sulfur atom in order to obtain the level of treatment we are achieving for dimers of **1**. In fact, it is likely that the use of sulfur DCPs, of a form similar to those of silicon,[9] would lead to overbinding in most of the thiophene dimers.

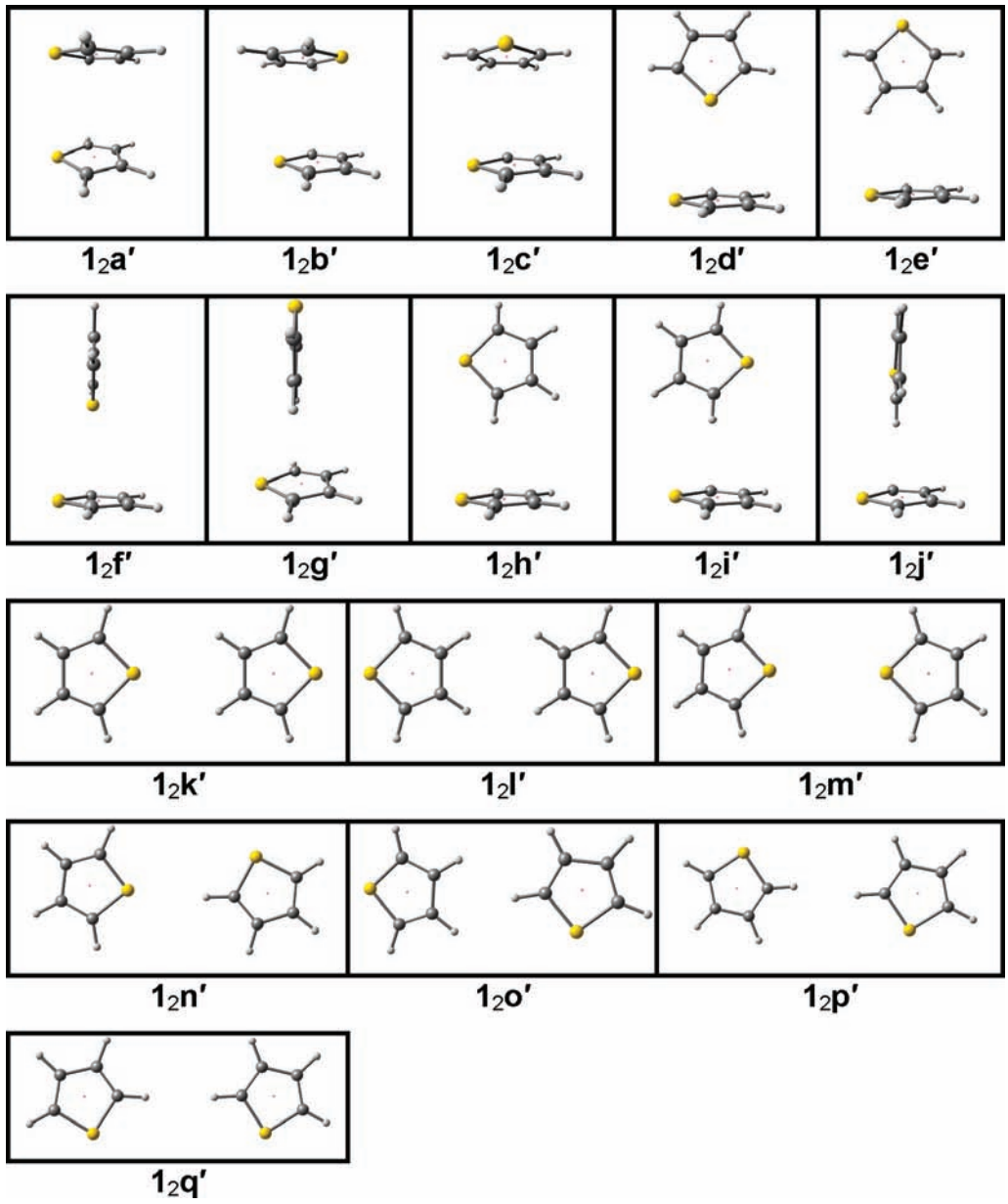

Figure 2. Perspective views of thiophene dimers $\mathbf{1}_2\mathbf{a}' - \mathbf{1}_2\mathbf{q}'$. These structures have been geometry optimized using B971/6-31+G(d,p)-DCP under the symmetry constraints described in ref 7. The small dot represents the ring centers of the thiophene monomers.

3. Results and Discussion

3.1. Thiophene (1) Dimers. Of the 17 dimers listed in Table 1, only 3 are energy minima with all positive frequencies − $\mathbf{1}_2\mathbf{e}$, $\mathbf{1}_2\mathbf{h}$, and $\mathbf{1}_2\mathbf{i}$ (equivalent to $\mathbf{1}_2\mathbf{e}'$, $\mathbf{1}_2\mathbf{h}'$, and $\mathbf{1}_2\mathbf{i}'$). These are all T-shaped in nature with C_s symmetry; see Figure 2. Distances between monomer geometric ring centers equal 4.90, 4.92, and 4.92 Å for $\mathbf{1}_2\mathbf{e}$, $\mathbf{1}_2\mathbf{h}$, and $\mathbf{1}_2\mathbf{i}$, respectively. These are in good agreement with the CCSD(T)-determined distances which give 4.8, 5.0, and 5.0 Å for the corresponding dimers. Bear in mind that these CCSD(T) numbers characterize the lowest energy single-point calculation at this level and are not fully optimized geometries. To quantify the potential energy landscape for $\mathbf{1}_2$ we removed the applied symmetry constraints and allowed the geometries to relax. The result was 11 true minima that purport to T-shaped or sandwich structures and one coplanar structure ($\mathbf{1}_2\mathbf{n}$). The binding energies for all of these structures, along with the three symmetry constrained dimers, are provided in the Supporting Information. The labeling we use for these optimized structures correlates with those used for the symmetry-constrained structures indicated in Table 1. However, dimers with similar labels do not necessarily have the same structural motif (vide infra).

The 10 T-shaped structures (see Supporting Information) show binding in the range 3.00 ($\mathbf{1}_2\mathbf{p}$) to 1.83 kcal/mol ($\mathbf{1}_2\mathbf{q}$). π-stacked dimer structures are bound in the range 2.54 ($\mathbf{1}_2\mathbf{a}$ and $\mathbf{1}_2\mathbf{l}$) to 2.20 kcal/mol ($\mathbf{1}_2\mathbf{c}$). See Figure 3 for pictures of the lowest energy T-shaped and π-stacked dimers.

It is important to highlight the effects on binding when the dimer structures are allowed to fully geometry optimize. The coplanar dimers reported in Table 1 are particularly unstable and our calculations predict that only one coplanar structure survives full structural relaxation.

The structure with the greatest binding is $\mathbf{1}_2\mathbf{p}$ (Figure 3a), with BE = 3.0 kcal/mol according to B971/6-31+G(d,p)-DCP.[29] This dimer has a T-shape with its monomer dipoles somewhat antialigned. The binding in $\mathbf{1}_2\mathbf{p}$ is 0.35 kcal/mol (ca. 15%) more than the largest binding found for the analogous T-shaped, symmetry-constrained dimer $\mathbf{1}_2\mathbf{i}'$. The most strongly

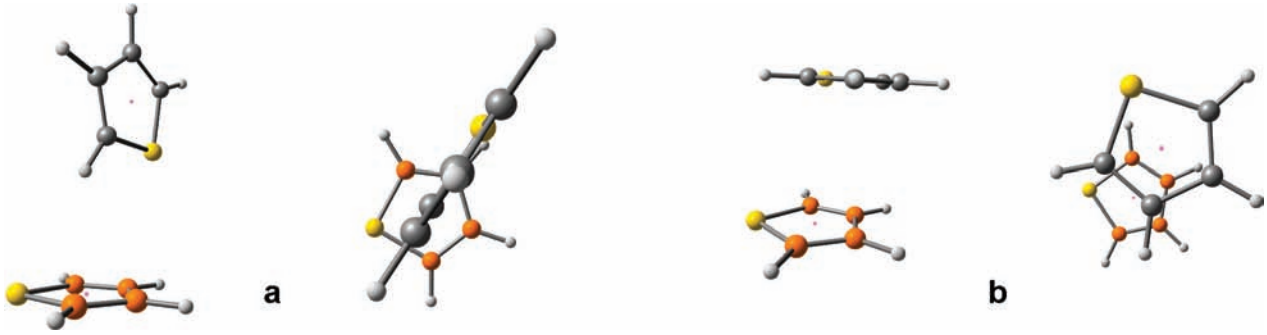

Figure 3. B971/6-31+G(d,p)-DCP optimized geometries for thiophene dimers (a) $\mathbf{1_2p}$ [BE = 3.0 kcal/mol] and (b) $\mathbf{1_2a}$ [BE = 2.54 kcal/mol]. Shown are two perspective views: side-on and from above. Carbon atoms of one monomer are colored orange for clarity. The small dot represents the ring centers of the thiophene monomers.

bound symmetry constrained π-stacked dimer ($\mathbf{1_2c'}$) has a BE of 1.67 kcal/mol. This increases by ca. 52% to 2.54 kcal/mol in $\mathbf{1_2a}$ (Figure 3b). This large change in BE is attributable to the ring slip that occurs with geometry relaxation. The T-shaped structures do not display such large structural changes upon full geometry optimization. These results show that BEs calculated for symmetry constrained geometries are qualitative, at best.

We inspected all of the dimer structures in order to assess the effect of dipole alignment in the π-stacked dimer structures. The result is that no definitive conclusions about the relationship between dipole alignment and BE can be provided. The expectation is that having dipoles antialigned (i.e., pointing in opposite directions) would confer greater binding between monomers. This appears to be the case for the T-shaped dimers. For example, $\mathbf{1_2p}$ (see Figure 3a) and $\mathbf{1_2d}$ (see the SI) have monomer dipoles that are nearly antialigned and have BEs = 3.0 kcal/mol, c.f. $\mathbf{1_2o}$ (see Supporting Information), which has monomer dipoles that are aligned and has a BE = 2.5 kcal/mol. However, the π-stacked structures $\mathbf{1_2l}$ and $\mathbf{1_2a}$, which have the same binding energies and almost equivalent distances between monomers, have their dipoles opposed.

In the extensively reported case of the benzene dimer there would seem to be general consensus that symmetric T-shaped and parallel-displaced (PD) structures are ca. isoenergetic. By use of the CCSD(T)/CBS values determined by Sherrill and co-workers[32] as an explicatory example, the binding for these species are 2.74 and 2.78 kcal/mol for T and PD structures, respectively. Contrast this to the difference in relative energies for the nonsymmetry constrained $\mathbf{1_2p}$ and $\mathbf{1_2a}$ (ca. 0.5 kcal/mol). This greater difference may, in part, be due to dipole effects evident in the thiophene dimer. However, as pointed out recently, the T-shaped benzene dimer is not an energy minimum, being instead a transition state.[33] The more favored structure is a tilted-T, which, according to the recent work of Hobza and co-workers,[34] is 0.09 kcal/mol most stable.[35] This benzene dimer is tilted out of the C_2 axis by ca. 7°. This tilt angle is the angle away from normal. In contrast, the thiophene dimer $\mathbf{1_2p}$ has a tilt angle of about 12°.

Clearly, dipole-related interactions must be considered in conjunction with dispersion attraction in order to obtain reliable estimates of dimer structures. Dispersion interactions may be large enough in some cases to overcome unfavorable dipole alignments in monomers. A good example of this is shown in Figure 1. Conventional DFT methods, that is, those that do not properly take into account dispersion interactions, will incorrectly predict dimer potential energy surfaces with minima dominated by dipole interactions (vide infra).

3.2. Benzothiophene (2) Dimers. Substitution of a benzene ring to the side of each thiophene monomer immediately results in π-stacked structures dominating the potential energy landscape. By use of the starting geometries of $\mathbf{1_2}$ described in the previous section, benzene moieties were added to the sides of each thiophene monomer to give a total of 26 unique local energy minima for $\mathbf{2_2}$. Fourteen dimers are sandwich structures with angles between ring planes of less than 10°. Four more dimers can be described as Ts (plane angles range 70−85°), while six lie somewhere in-between these characteristics and are thus henceforth referred to as tilted-Ts. These tilted-Ts show angles between planes of between 10 and 63°. Only two coplanar dimers exist. The binding energies of the most strongly bound dimers representing each of the structural motifs are given, along with pictures of the structures and other structural information, in Figure 4. Pictures and BEs of all structures can be found in Supporting Information. We label each structure in a similar fashion to that for $\mathbf{1_2}$, such that an attempt is made to relate each to the symmetry constrained starting point of $\mathbf{1_2}$. However, in some instances this is not appropriate and therefore these structures are labeled from $\mathbf{2_2r}$ onward. From the $\mathbf{1_2}$ starting structures, a benzene moiety can be added to either end of a thiophene monomer so as to provide two initial $\mathbf{2_2}$ structures that are subjected to geometry optimization; these are labeled accordingly with a suffix "i" or "ii".

Greatest binding, 5.8 kcal/mol, is found for $\mathbf{2_2k_{ii}}$. This species, as shown in Figure 4a, is a slipped-parallel-type structure with thiophene moiety over thiophene moiety and benzene moiety over benzene moiety. The dipoles of the thiophene moieties are antialigned. $\mathbf{2_2h_{ii}}$ is similar to $\mathbf{2_2k_{ii}}$ except that its dipoles are closer to aligned. This minima is 0.2 kcal/mol higher in energy than $\mathbf{2_2k_{ii}}$. The greater binding in $\mathbf{2_2k_{ii}}$ is a result of the more favorable dipole alignment compared to $\mathbf{2_2h_{ii}}$.

Of the tiled-Ts, $\mathbf{2_2k_i}$ (Figure 4b) shows the largest degree of binding, lying at 5.1 kcal/mol. Labeling $\mathbf{2_2k_i}$ as being tilted-T may seem incongruous, given the views shown in Figure 4b, but we would direct the reader to its optimized coordinates in SI in order to get a more realistic perspective on its configuration. The angle between ring planes in this structure is ca. 12°, thus relatively far from planar. This becomes clear when viewed in 3D. Interestingly, without the use of DCPs, this structure resorts toward a more regular T-shape (angle 87.6°) with one H pointed over the center of the benzene moiety and another pointed over the S atom in the second monomer.

As the tilt angle is increased toward a more regular T-shape, the binding decreases. This is illustrated with structures $\mathbf{2_2k_i}$, $\mathbf{2_2d_{ii}}$, $\mathbf{2_2e_i}$, $\mathbf{2_2d_i}$, and $\mathbf{2_2r_i}$, which have BEs (kcal/mol)/angles (deg) of ca. 5.1/12, 4.7/16, 4.2/41, 4.0/63, and 3.6/60, respectively (see Supporting Information). This is likely attributable to decreasing contact area or monomer overlap as the tilt angle increases.

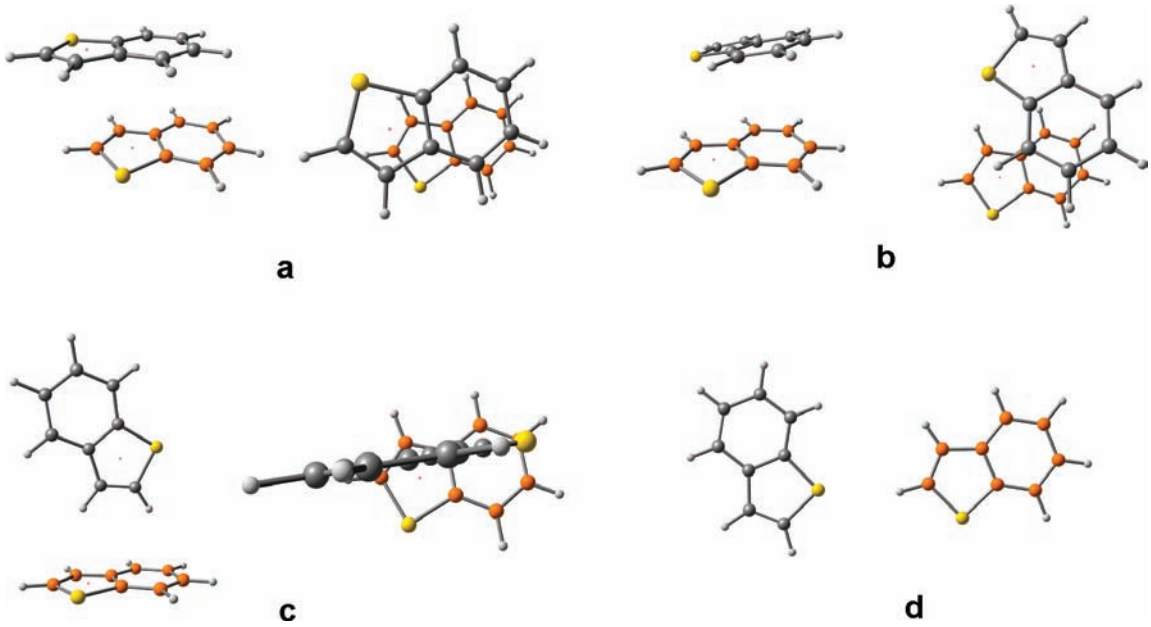

Figure 4. B971/6-31+G(d,p)-DCP optimized geometries for benzothiophene dimers. Structural motif, binding energies, thiophene ring-center separations and plane angles are given in kcal/mol, Å, and degrees, respectively. (a) $\mathbf{2_2k_{ii}}$: π-stacked, BE = 5.8, distance = 3.84, angle = 1.6. (b) $\mathbf{2_2k_i}$: tilted-T-shaped, BE = 5.1, distance = 3.75, angle = 11.9. (c) $\mathbf{2_2i_i}$: T-shaped, BE = 4.1, distance = 4.79, angle = 79.0. (d) $\mathbf{2_2n_{ii}}$: coplanar, BE = 0.8, distance = 6.83, angle = 0.0. Shown for the dimers other than coplanar are perspective views side-on and from above. Carbon atoms of one monomer are colored orange for clarity.

T-shaped structures of $\mathbf{2_2}$ show binding in the range 4.1−3.8 kcal/mol. The T-shaped structure with greatest binding, $\mathbf{2_2i_i}$ (Figure 4c) has a BE that is 1.7 kcal/mol lower than $\mathbf{2_2k_{ii}}$ (Figure 4a) and 0.7 kcal/mol lower than that of $\mathbf{2_2c_i}$. $\mathbf{2_2k_{ii}}$ and $\mathbf{2_2c_i}$ represent the range of binding in the π-stacked dimer structures. Therefore, $\mathbf{2_2i_i}$ has a lower BE than the most weakly bound π-stacked dimer.

As is the case for the thiophene dimers, coplanar structures have BEs less than 1 kcal/mol. $\mathbf{2_2n_{ii}}$, shown in Figure 4d, is bound by 0.8 kcal/mol, which is only 0.03 kcal/mol lower in energy than its related $\mathbf{2_2n_i}$. Both structures contain C_s symmetry.

Tsuzuki et al.[7] show that while dispersion interactions are of primary importance to the attraction in all thiophene dimers, the dominance is particularly keenly felt in the π-stacked case. That being the case and by consideration that the T-shaped dimers contain more prevalent dipole-related binding interactions, then the tilted-T-shaped dimers neatly demonstrate the interplay of dispersion binding and dipole effects. The greater binding energies for the π-stacked geometries of $\mathbf{2_2}$ suggests that these forces dominate over any dipole−induced dipole interactions evident in T-stacked dimers, as a result of the greatly increased contact area compared to the simpler thiophene dimer, $\mathbf{1_2}$.

3.3. Dibenzothiophene (3) Dimers. Adding two benzenes to either side of the thiophene monomer results in dibenzothiophene, **3**. Given the much reduced binding observed in any coplanar isomer of both $\mathbf{1_2}$ and $\mathbf{2_2}$, we did not search for structures with this motif for the present $\mathbf{3_2}$ case or for the proceeding $\mathbf{4_2}$ dimers. Ten different minimum energy structures have been determined using the $\mathbf{1_2a'}-\mathbf{1_2j'}$ structures as starting points.

In this case, only one structure relaxes to a regular T shape, with an angle of 88.3° between monomer planes. One further structure is tilted-T-shaped (angle 11.0°). The remaining structures all have angles less than 10°. The binding energies, angles, and distances between geometric ring centers and pictures for all dimer structures can be found in Supporting Information. This result indicates that dispersion interactions are far more dominant than dipole-related interactions.

The structure with the largest binding energy (9.0 kcal/mol) is $\mathbf{3_2i}$, see Figure 5a. This corresponds to a π-stacking motif with dipoles antialigned. The thiophene and benzene moieties are slipped and rotated relative to one another, and hence the monomers are not perfectly cofacial. Increasing the degree of slipping and rotation between the monomers in a π-stacked dimer reduces the $\pi-\pi$ overlap and the overall binding. This can be seen for $\mathbf{3_2j}$ (see Supporting Information), which has the largest degree of slippage/rotation and the weakest binding (BE = 7.5 kcal/mol).

The $\mathbf{3_2d}$ structure (BE = 3.0 kcal/mol, Figure 5b) has much lower binding energy than the other structures as can be understood from the lack of π overlap. This T-shaped structure has an angle between monomer planes that is close to 90° and thus does not exhibit the stabilizing tilting seen in the most stable benzothiophene structure ($\mathbf{2_2i_i}$).

What is clear from the structures determined is that there are no tilted-T structures that possess angles in the region 16−70°, as found for **2**. The tilt angle of 11° (observed in $\mathbf{3_2e}$, see Figure 5c) can be said to be the mostly strongly bound tilted-T type dimer structure. Interestingly, this structure can also be described as "crossed", where one monomer is rotated nearly 90° with respect to the other. This will necessarily reduce $\pi-\pi$ overlap between the monomers and may influence the degree of tilting between monomer planes.

The experimentally[36] determined dipole moment of dibenzothiophene (0.88 D)[36] is marginally greater than that of benzothiophene (0.84 D).[36] However, the increasing domination of π-stacking over other favorable interactions is evidenced here. The difference in binding energy between the most stable π-stacked dimer and the most stable T-shaped is ca. 6 kcal/mol. The decided lack of any great number of tilted-T-shaped dimers that are prevalent for $\mathbf{2_2}$ also points to greater supremacy of the $\pi-\pi$ interaction over all others.

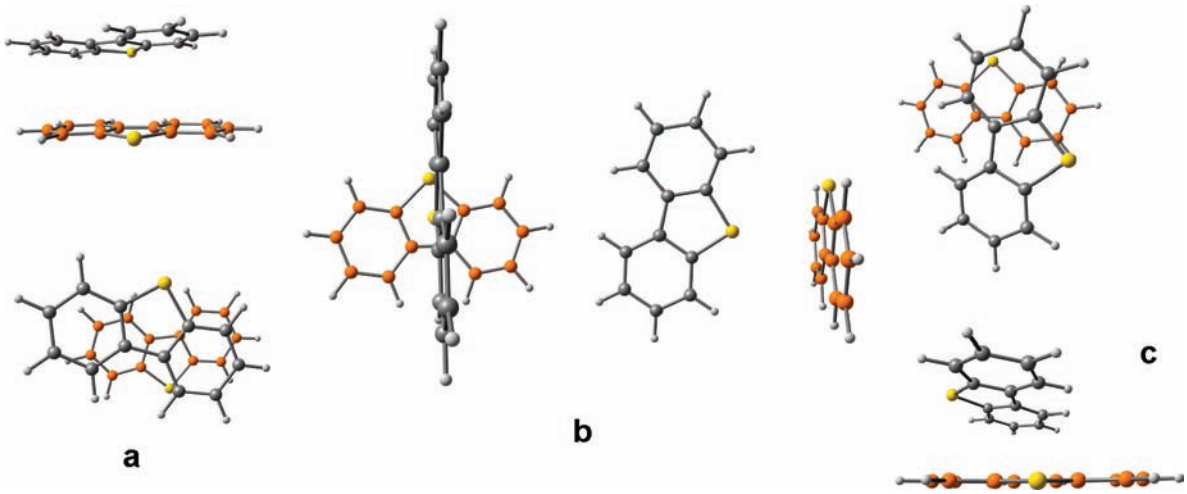

Figure 5. B971/6-31+G(d,p)-DCP optimized geometries for dibenzothiophene dimers. Structural motif, binding energies, thiophene ring-center separations, and plane angles are given in kcal/mol, Å, and degrees, respectively. (a) $\mathbf{3_2i}$: π-stacked, BE = 9.0, angle = 4.5, distance = 4.1; (b) $\mathbf{3_2d}$: T-shaped, BE = 3.0, angle = 88.3, distance = 5.0; (c) $\mathbf{3_2e}$: tilted-T-shaped, BE = 8.5, angle = 11.0, distance = 4.5. Shown are perspective views side-on and from above. Carbon atoms of one monomer are colored orange for clarity.

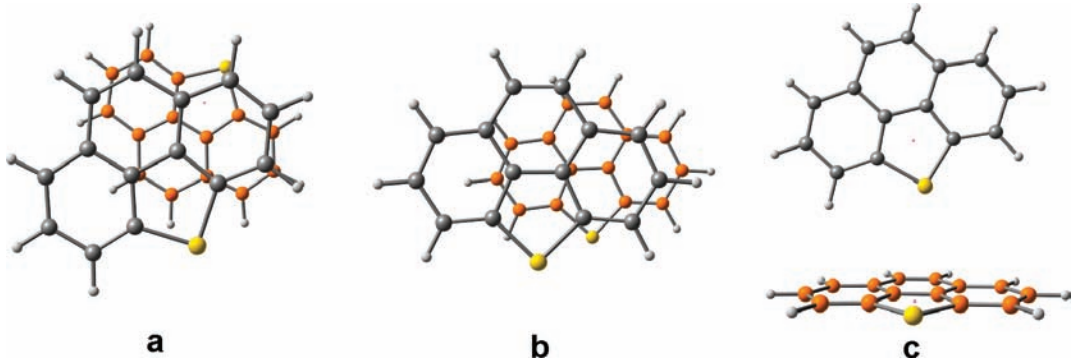

Figure 6. B971/6-31+G(d,p)-DCP optimized geometries for tribenzothiophene dimers. Structural motif, binding energies, thiophene ring-center separations and plane angles are given in kcal/mol, Å, and degrees, respectively. (a) $\mathbf{4_2j_i}$: π-stacked, BE = 11.0, angle = 1.8, distance = 4.8; (b) $\mathbf{4_2a}$: π-stacked, BE = 10.6, angle = 0.7, distance = 3.9; (c) $\mathbf{4_2d_{ii}}$: T-shaped, BE = 4.3, angle = 88.1, distance = 5.0. Carbon atoms of one monomer are colored orange for clarity.

3.4. Tribenzothiophene (4) Dimers. We report the structures of 11 dimers of tribenzothiophene ($\mathbf{4_2}$) with their binding energies in Supporting Information. The structures, BEs, and structural information for representative π-stacked and T-shaped structures are given in Figure 6. The starting geometries for the subsequent optimizations were created by the addition of benzene rings to the sides of each thiophene monomer as previously described for dimers $\mathbf{2_2}$ and $\mathbf{3_2}$. Further starting geometries were derived for the T-shaped dimers by moving the leg of the T along the plane of the arm so as to maximize point contact between monomers. In these instances suffixes are used to distinguish the parent isomer (suffix i) to its related starting geometries.

The majority, 9, of the optimized geometries are slipped parallel, π-stacked structures with only two T-shaped dimers found. No tilted-T structures have been determined for this species. π-stacked dimers are shown to bind with energies in the range 11.0−9.3 kcal/mol. Two of these are $\mathbf{4_2j_i}$ and $\mathbf{4_2a}$ (parts a and b of Figure 6, respectively). In contrast, the two T-shaped dimers ($\mathbf{4_2d_i}$ and $\mathbf{4_2d_{ii}}$) are bound by 4.3 and 3.9 kcal/mol, viz., by less than half the strength compared to the π-stacked species. This is not surprising given that we have previously found similarly extensive differences for other large hydrocarbon dimers. For example, for hexabenzocoronene, there is a 4-fold difference in binding between sandwich and T-shaped dimers.[8]

Parts a and b of Figure 6 show just two of the numerous $\pi-\pi$ stacked dimers. $\mathbf{4_2j_i}$ (Figure 6a) is the lowest energy isomer of $\mathbf{4_2}$ with a binding energy of 11.0 kcal/mol. This structure has the monomer dipoles in a perpendicular orientation. $\mathbf{4_2a}$ (Figure 6b) is 0.4 kcal/mol higher in energy and has aligned dipoles.

For the T-shaped dimers, greater binding is observed when there is greatest point contact between monomers. $\mathbf{4_2d_{ii}}$ is ca. 0.3 kcal/mol more bound than $\mathbf{4_2d_i}$. The structure of $\mathbf{4_2d_{ii}}$, as seen in Figure 6c is such that the upright monomer shown is tilted out of the vertical axis to afford a CH$\cdots\pi$ interaction between benzene moieties.

3.5. Interactions between Monomers. Examination of the $\mathbf{4_2}$ π-stacked structures might lead one to believe that the greatest binding is found when there exists **1**−benzene interactions rather than **1**−**1** interactions. For example, see $\mathbf{4_2j_i}$ (Figure 6a, BE = 11.0 kcal/mol) compared to $\mathbf{4_2c}$ (see Supporting Information, BE = 9.3 kcal/mol). However, for the simpler cases of $\mathbf{1_2}$ and **1** bound to benzene (see Supporting Information), there is no difference in binding for π-stacked structures. That is, BE ($\mathbf{1_2a}$) = 2.5 kcal/mol (see Figure 3b) is the same as that of the lowest energy π-stacked dimer of **1**−benzene. This contrasts with the recently published CCSD(T)-level data of Hohenstein and Sherrill[37] on the benzene-pyridine and pyridine dimers, which have the latter ca. 0.7 kcal/mol more stable.

For the benzothiophene dimer $\mathbf{2_2k_{ii}}$, which is the lowest energy structure of this family (BE = 5.8 kcal/mol), benzene lies over benzene and thiophene lies over thiophene in a slipped parallel fashion. This structure is 0.1 kcal/mol lower in energy than when benzene moieties overlap and thiophenes overlap, as in $\mathbf{2_2l_i}$. In other words, there appears to be very little difference in π-stacking interactions in the case where the nearest interacting ring systems are both nonpolar compared to the case where one of the pair of interacting rings is polar. However, it is possible that similarities in **1**−benzene and **1**−**1** binding may reflect dipole−induced dipole effects in the former being of the same magnitude of dipole−dipole interactions in the latter.

The dipole moments of **1**, **2**, and **3** are known experimentally[36] to increase from 0.54 to 0.84 to 0.88 D, respectively. However, as shown in the previous sections, we find that π-stacking interactions quickly become dominant through this series (and following on to **4**), somewhat negating the effect of dipole interactions on these dimers. It is also interesting to note that the most strongly bound T-shaped dimers for **2** show the monomer dipoles to lie ca. perpendicular to each other, while for $\mathbf{3_2}$ and $\mathbf{4_2}$ the S atom of one monomer is directed toward the center of the heteroatomic ring of the other monomer. Therefore, dipole effects play a very small role in determining the structure of these dimers.

The presence of tilted-T-shaped dimers for $\mathbf{2_2}$ (and to a lesser extent $\mathbf{3_2}$) but not for $\mathbf{4_2}$ may have implications to the modeling of organic molecular electronics, and the design thereof. In the latter case the amount of $\pi-\pi$ overlap is so extensive that a more planar dimer dominates. For $\mathbf{2}_2$ there appears to be a more noticeable contribution of both dipole and π-stacking interactions to the observed binding.

3.6. Importance of Dispersion Effects. The use of DCPs allows for the switching on and off of dispersion treatment. To examine the extent of the importance of dispersion to the structure determination of dimers $\mathbf{1}_2-\mathbf{4}_2$, we briefly discuss here the effect on structure and binding energy when DCPs are not used in the calculations. The reader is referred to the SI section for complete details of how dispersion influences the structure and binding energies of the dimers.

In the case of $\mathbf{1}_2$, the main observation is that three of the four π-stacked dimers found with DCPs become T-shaped dimers when dispersion is not included. Not surprisingly, the binding energies for those dimers with comparable structural motifs are substantially reduced when dispersion is not included, viz., by 10−67%.

For dimers of **2**, only a few of the π-stacked dimers undergo a change in structural motif when dispersion is switched off. However, in the absence of DCPs, many of the π-stacked dimers optimize to saddle points on the respective potential energy surface. In cases such as these, we did not perform additional computations to ascertain the ultimate structures of these dimers. We also found that about two-thirds of the tilted-T $\mathbf{2_2}$ structures become T-shaped dimers when DCPs are removed. The BEs of $\mathbf{2_2}$ drop by ca. 25−80% when DCPs are not included in the calculations.

Similar results are found for $\mathbf{3}_2$, in which five out of eight π-stacked dimers converge toward a T-shape structure and the tilted-T dimers become more regular T structures when dispersion is not included. Therefore, the potential energy surface of $\mathbf{3_2}$ is dominated by π-stacked dimers when dispersion is included but by T-shaped structures in the absence of dispersion corrections. The BEs for $\mathbf{3}_2$ structures are also reduced by up to 80% when dispersion is not included.

Interestingly, for $\mathbf{4_2}$ we do not find such discrepancy between DCP and non-DCP structural motifs. However, in this case, as in all of the dimers studied, the lack of dispersion correction seriously underestimates the observed binding energies: For $\mathbf{4_2}$, BEs are underestimated by up to 80% when DCPs are not included. This amounts to a discrepancy of ca. 8.3 kcal/mol in the binding of $\mathbf{4_2j_i}$, which is the most strongly bound π-stacked structure we found for dimers of **4**.

4. Summary

We have used a newly developed dispersion-corrected density functional theory approach to study the noncovalent binding associated with dimerization of thiophene (**1**), and of mono (**2**), di (**3**), and tribenzothiophene (**4**). The dispersion correction involves the use of simple, carbon atom-centered potentials termed dispersion-correcting potentials or DCPs. Thiophenes of the type studied in this work are of interest in petrochemistry and in organic electronics, and understanding their noncovalent interactions are important for developing insights into their material properties. Our approach was benchmarked against the high-level ab initio data reported by Tsuzuki et al.[7]

Dimerization of **1** can result in a large number of energetically low-lying structures. We found 15 minima in total. Ten of these structures have a T-shaped motif, while four have a π-stacked structure, and one dimer has the monomers coplanar. Dipole−induced dipole interactions, which are prevalent in T-shaped structures, therefore have a strong influence on the potential energy surface of dimers of **1**. The most strongly bound T-shaped dimer has a binding energy, BE, of 3.0 kcal/mol and monomer dipoles approximately antialigned. The lowest-lying π-stacked structure has a BE = 2.5 kcal/mol and has monomer dipoles approximately aligned. The dimer structure in which the monomers are coplanar has a much lower binding energy - less than 0.7 kcal/mol.

For dimers of **2**, 26 minimum energy structures were found. The lowest energy structure in this case is a π-stacked structure with BE = 5.8 kcal/mol. The most stable T-shaped structure has binding of 4.1 kcal/mol. A low-lying dimer complex with a structure motif that is intermediate to π-stacked and T, a so-called tilted-T structure, has a BE = 5.1 kcal/mol. This structure demonstrates the interplay between dispersion ($\pi-\pi$) binding and dipole−induced dipole interactions (T-shaped structures).

The potential energy landscape for dimers of **3** and **4** are dominated by π-stacked structures and therefore by dispersion interactions. The energetically lowest lying structures have binding energies of 9.0 and 11.0 kcal/mol for dimers of **3** and **4**, respectively. For both cases, T-shaped structures have BEs that are less than half of those of the π-stacked structures.

These results show that dispersion interactions, which are especially important in π-stacked structures, quickly dominate over dipole-induced and dipole−dipole forces as the size of the thiophene monomer increases. This result should be general for many other related systems, including larger polyaromatic asphaltenic systems and polythiophenes.

Our calculations revealed that many of the π-stacked structures studied revert to T-shaped structures, and binding energies are reduced by up to 80% when dispersion interactions are not included in the computations. Therefore, the correct description of the potential energy surfaces of the dimers under investigation depends on a reasonable treatment of dispersion interactions in conjunction with density functional theory. Clearly, the correction of the erroneous long-range behavior of density functional theory, as achieved through the use of DCPs, is essential to

determine all isomers of these dispersion bound dimers and thus sufficiently characterize these species.

Acknowledgment. We thank the Centre of Excellence for Integrated Nanotools, Academic Information and Communication Technologies, and Professor Pierre Boulanger all at the University of Alberta and WestGrid for access to computing resources. We also thank the Program for Energy Research and Development for funding.

Note Added after ASAP Publication. This paper was published on the Web on April 9, 2009. Due to production error, several typographical errors were corrected after initial Web posting. The corrected version was reposted on April 10, 2009.

Supporting Information Available: Optimized Cartesian coordinates and binding energies with full tables. This information is available free of charge via the Internet at http://pubs.acs.org.

References and Notes

(1) Murgich, J.; Abanero, J. A.; Strausz, O. P. *Energy Fuels* **1999**, *13*, 278–286.
(2) Hamedi, M.; Forchheimer, R.; Inganäs, O. *Nat. Mater.* **2007**, *6*, 357–362.
(3) Li, D.; Kaner, R. B. *Science* **2008**, *320*, 1170–1171.
(4) Mattheus, C. C.; de Wijs, G. A.; de Groot, R. A.; Palstra, T. T. M. *J. Am. Chem. Soc.* **2003**, *125*, 6323–6330.
(5) Hunter, C. A.; Sanders, J. K. M. *J. Am. Chem. Soc.* **1990**, *112*, 5525–5534.
(6) DiLabio, G. A. *Chem. Phys. Lett.* **2008**, *455*, 348–353.
(7) Tsuzuki, S.; Honda, K.; Azumi, R. *J. Am. Chem. Soc.* **2002**, *124*, 12200–12209.
(8) Mackie, I. D.; DiLabio, G. A. *J. Phys. Chem. A* **2008**, *112*, 10968–10976.
(9) Johnson, E. R.; DiLabio, G. A. *J. Phys. Chem. C*, DOI: 10.1021/jp8105056.
(10) Johnson, E. R.; DiLabio, G. A. *Chem. Phys. Lett.* **2006**, *419*, 333–339.
(11) Zhao, Y.; Truhlar, D. G. *Theor. Chem. Acc.* **2008**, *120*, 215–241.
(12) Dion, M.; Rydberg, H.; Schröder, E.; Langreth, D. C.; Lundqvist, B. I. *Phys. Rev. Lett.* **2004**, *92*, 246401.
(13) Iikura, H.; Tsuneda, T.; Yanai, T.; Hirao, K. *J. Chem. Phys.* **2001**, *115*, 3540–3544.
(14) Chai, J.-D.; Head-Gordon, M. *J. Chem. Phys.* **2008**, *128*, 084106.
(15) Grimme, S. *J. Comput. Chem.* **2004**, *25*, 1463–1473.
(16) Efforts to incorporate dispersion in similar ways are shown in the recent works: (a) Wodrich, M. D.; Jana, D. F.; Schleyer, P. v. R.; Corminboeuf, C. *J. Phys. Chem. A* **2008**, *112*, 11495–11500. (b) Sun, Y. Y.; Kim, Y.-H.; Lee, K.; Zhang, S. B. *J. Chem. Phys.* **2008**, *129*, 154102.
(17) Johnson, E. R.; Becke, A. D. *J. Chem. Phys.* **2005**, *123*, 024101.
(18) (a) von Lilienfeld, O. A.; Tavernelli, I.; Rothlisberger, U.; Sebastiani, D. *Phys. Rev. Lett.* **2004**, *93*, 153004. (b) von Lilienfeld, O. A.; Tavernelli, I.; Rothlisberger, U.; Sebastiani, D. *Phys. Rev. B* **2005**, *71*, 195119. (c) Lin, I.-C.; Coutinho-Neto, M. D.; Felsenheimer, C.; von Lilienfeld, O. A.; Tavernelli, I.; Rothlisberger, U. *Phys. Rev. B* **2007**, *75*, 205131. (d) Aeberhard, P. C.; Arey, J. S.; Lin, I.-C.; Rothlisberger, U. *J. Chem. Theory Comput.* **2009**, *5*, 23–28.
(19) Goedecker, S.; Teter, M.; Hutter, J. *Phys. Rev. B* **1996**, *54*, 1703–1710.
(20) DiLabio, G. A.; Hurley, M. M.; Christiansen, P. A. *J. Chem. Phys.* **2002**, *116*, 9578–9584.
(21) Moon, S.; Christiansen, P. A.; DiLabio, G. A. *J. Chem. Phys.* **2004**, *120*, 9080–9086.
(22) DiLabio, G. A.; Dogel, S. A.; Wolkow, R. A. *Surf. Sci.* **2006**, *600*, L209−L213.
(23) Frisch, M. J.; Trucks, G. W.; Schlegel, H. B.; Scuseria, G. E.; Robb, M. A.; Cheeseman, J. R.; Montgomery, J. A., Jr.; Vreven, T.; Kudin, K. N.; Burant, J. C.; Millam, J. M.; Iyengar, S. S.; Tomasi, J.; Barone, V.; Mennucci, B.; Cossi, M.; Scalmani, G.; Rega, N.; Petersson, G. A.; Nakatsuji, H.; Hada, M.; Ehara, M.; Toyota, K.; Fukuda, R.; Hasegawa, J.; Ishida, M.; Nakajima, T.; Honda, Y.; Kitao, O.; Nakai, H.; Klene, M.; Li, X.; Knox, J. E.; Hratchian, H. P.; Cross, J. B.; Bakken, V.; Adamo, C.; Jaramillo, J.; Gomperts, R.; Stratmann, R. E.; Yazyev, O.; Austin, A. J.; Cammi, R.; Pomelli, C.; Ochterski, J. W.; Ayala, P. Y.; Morokuma, K.; Voth, G. A.; Salvador, P.; Dannenberg, J. J.; Zakrzewski, V. G.; Dapprich, S.; Daniels, A. D.; Strain, M. C.; Farkas, O.; Malick, D. K.; Rabuck, A. D.; Raghavachari, K.; Foresman, J. B.; Ortiz, J. V.; Cui, Q.; Baboul, A. G.; Clifford, S.; Cioslowski, J.; Stefanov, B. B.; Liu, G.; Liashenko, A.; Piskorz, P.; Komaromi, I.; Martin, R. L.; Fox, D. J.; Keith, T.; Al-Laham, M. A.; Peng, C. Y.; Nanayakkara, A.; Challacombe, M.; Gill, P. M. W.; Johnson, B.; Chen, W.; Wong, M. W.; Gonzalez, C.; Pople, J. A. *Gaussian 03*, revision D.01; Gaussian, Inc.: Wallingford, CT, 2004.
(24) Becke, A. D. *J. Chem. Phys.* **1993**, *98*, 5648–5652.
(25) Lee, C.; Yang, W.; Parr, R. G. *Phys. Rev. B* **1988**, *37*, 785–789.
(26) Hamprecht, F. A.; Cohen, A. J.; Tozer, D. J.; Handy, N. C. *J. Chem. Phys.* **1998**, *109*, 6264–6271.
(27) Perdew, J. P.; Burke, K.; Ernzerhof, M. *Phys. Rev. Lett.* **1996**, *77*, 3865–3868.
(28) Without DCPs these structures relax to T-shaped dimers, similar in structure to **1_2p**.
(29) As a check we computed the BE for this structure (using the B971/6-31+G(d,p)-DCP-optimized monomer and dimer structures) using an estimated CCSD(T)/CBS approach we have used in the past. The procedure used can be summarized as follows: (1) Single-point energies are calculated using counterpoise-corrected,[30] MP2/aug-cc-pVQZ and MP2/aug-cc-pVTZ; (2) CBS extrapolated energies, E_{CBS}, are determined with the MP2 energies from 1 using the extrapolation scheme described in ref 31; (3) the extrapolation correction, ΔE_{extrap}, is determined by subtracting E(MP2/aug-cc-pVTZ) from E_{CBS}; (4) the final system energy is determined by summing counterpoise-corrected, E(CCSD(T)/aug-cc-pVTZ and ΔE_{extrap}. Energies so obtained for the monomer and dimer species are used to obtain a BE = 3.5 kcal/mol for **1_2p**: Our DCP-derived BE is within ca. 14% of this value.
(30) Boys, S. B.; Bernardi, F. *Mol. Phys.* **1970**, *19*, 553–556.
(31) Martin, J. M. L. *Chem. Phys. Lett.* **1996**, *259*, 669–678.
(32) Sinnokrot, M. O.; Valeev, E. F.; Sherrill, C. D. *J. Am. Chem. Soc.* **2002**, *124*, 10887–10893.
(33) (a) DiStasio, R. A., Jr.; von Helden, G.; Steele, R. P.; Head-Gordon, M. *Chem. Phys. Lett.* **2007**, *437*, 277–283. (b) Lee, E. C.; Kim, D.; Jureèka, P.; Tarakeshwar, P.; Hobza, P.; Kim, K. S. *J. Phys. Chem. A* **2007**, *111*, 3446–3457.
(34) Pitoňák, M.; Neogrády, P.; Řezáč, J.; Jurečka, P.; Urban, M.; Hobza, P. *J. Chem. Theory Comput.* **2008**, *4*, 1829–1834.
(35) See footnote g of Table 3 of ref 34.
(36) (a) Bak, B.; Christensen, D.; Hansen-Nygaard, L.; Rastrup-Andersen, J. *J. Mol. Spectrosc.* **1961**, *7*, 58–63. (b) Charles, R. G.; Freiser, H. *J. Am. Chem. Soc.* **1950**, *72*, 2233–2235. (c) Gruntfest, M G.; Kolodyazhnyi, Y. V.; Udre, V. É.; Voronkov, M. G.; Osipov, O. A. *Chem. Heterocycl. Compd.* **1970**, *6*, 413–415.
(37) Hohenstein, E. G.; Sherrill, C. D. *J. Phys. Chem. A* **2009**, *113*, 878–886.

JP901001W